Adipose tissue-derived mesenchymal stem cells attenuate lung inflammation and fibrosis in the bleomycin-induced pulmonary fibrosis rat model via caveolin-1/NF-kB signaling axis

Zhe Chen[1], Bingqing Ruan[2], Guangyan Long[3], Wei Lin[4, #]

Running title: ADMSCs attenuate PF

[1]Department of Respiratory and Critical Care Medicine, The First People's Hospital of Wenling, Zhejiang 317500, China.

[2]Department of Internal Medicine, Wenling Women's and Children's Hospital, Zhejiang 317500, China.

[3]Department of Infectious Disease, The First People's Hospital of Wenling, Zhejiang 317500, China.

[4]Department of Respiratory, The First People's Hospital of Wenling, Zhejiang 317500, China.

[#]Corresponding author: Mr. Wei Lin. Department of Respiratory, The First People's Hospital of Wenling, 333 Chuanan South Road, Wenling, Zhejiang 317500, China. Email: wenlwe_lin@hotmail.com. ORCID: 0000-0002-0411-5468

Summary

Stem cells have emerged as promising therapeutic options for several human diseases, including pulmonary fibrosis (PF). In this study, we investigated the therapeutic effects of adipose tissue-derived mesenchymal stem cells (ADMSCs) in the bleomycin-induced PF model rats and the underlying mechanisms. The PF model rats were generated by intratracheal injections of 5mg/kg bleomycin sulfate. The ADMSC group rats were generated by injecting 2.0×10^6 ADMSCs via the tail vein at 0, 12, and 24 h after bleomycin injection. The control, PF, and ADMSC group rats were sacrificed on day 21 after bleomycin injections and the changes in lung histology and the levels of pro-inflammatory cytokines, collagen I, and caveolin-1 (Cav-1), and the activity of the NF-κB signaling pathway in the lung tissues was assessed by hematoxylin-eosin staining, ELISA, and western blotting assays. The lung tissues of the PF model rats showed significant infiltration of neutrophils, tissue destruction, and collagen deposition, but these effects were abrogated by the ADMSCs. The levels of pro-inflammatory cytokines such as IL-6, IL-1β, and TGF-β1 were elevated in the lung tissues and the bronchoalveolar lavage fluid (BALF) of the bleomycin-induced PF model rats, but these effects were reversed by the ADMSCs. The lung tissues of the PF model rats showed significant downregulation of Cav-1 and significantly higher activation of the pro-inflammatory NF-κB pathway. However, administration of the ADMSCs restored the expression levels of Cav-1 and suppressed the NF-κB signaling pathway in the lungs of the bleomycin-induced PF model rats. In conclusion, this study demonstrated that the ADMSCs protected against bleomycin-induced PF in the rat model by modulating the Cav-1/ NF-κB axis.

Keywords: adipose tissue-derived mesenchymal stem cell; caveolin-1; inflammation; NF-κB; pulmonary fibrosis.

Abbreviations

PF: Pulmonary fibrosis

CF: Cystic fibrosis

PH: Pulmonary hypertension

ARDS: Acute respiratory distress syndrome

ADMSC: Adipose-derived mesenchymal stem cell

ESC: Embryonic stem cells

BMSC: Bone marrow mesenchymal stem cell

Introduction

Pulmonary fibrosis (PF) is a chronic lung disease characterized by the progressive accumulation of extracellular matrix and remodeling of the lung architecture and reduced lung function [1, 2], which leads to exertional dyspnea with limitations of ordinary tasks [3]. The mortality rate of PF patients is about 40%. Furthermore, the increasing incidence rates of PF is significantly burdening the public health systems worldwide. Currently, the primary therapeutic strategy for PF includes treatment with immunosuppressive drugs such as prednisone, azathioprine or cyclophosphamide [4]. However, the treatment outcomes of the immunosuppressive drugs are not satisfactory and are associated with significant adverse effects [5]. Thus, the anti-inflammatory drugs are still preferred for treating patients with PF because they attenuate collagen deposition [6] and suppress the epithelial and vascular injury in the lungs [7]. There is an urgent need for the development of effective treatment strategies for ameliorating pulmonary damage by suppressing both inflammation and fibrosis in the patients with PF.

Stem cell-based therapy is a promising approach for the treatment of several lung diseases such as cystic fibrosis (CF), pulmonary hypertension (PH), and acute respiratory distress syndrome (ARDS) [8]. Ortiz et al. demonstrated that the engraftment of mesenchymal stem cells (MSCs) attenuated bleomycin-induced lung inflammation and fibrosis in a murine model by homing to the site of injury and adopting an epithelium-like phenotype [9]. Periera-Simon et al demonstrated anti-fibrotic effects (decreased Ashcroft score and hydroxyproline levels) of the human MSCs derived from various sources such as the adipose tissues, Wharton's jelly (WJ), chorionic membranes (CSCs), and the chorionic villi (CVC) in an ageing mouse model of BLM-induced lung fibrosis [10]. In comparison with the embryonic stem cells (ESCs) and the bone marrow mesenchymal stem cells (BMSCs), adipose-derived mesenchymal stem cells (ADMSCs) show significant advantages as the source of MSCs for stem cell therapy because of their abundance, accessibility without the use of invasive techniques, and the requirement of easy culturing conditions [11]. Banas et al. reported that the therapeutic efficacy of the ADMSCs was significantly higher than the bone marrow-derived stem cells (BMSCs) and normal human dermal fibroblasts (NHDFs) in treating liver injury [12]. Therefore, ADMSCs represent a promising cost-effective treatment approach for treating PF with fewer side effects.

The mechanisms underlying the beneficial effects of ADMSCs in the treatment of PF are not clear. Several PF-related molecules that play a role in the pathogenesis and progression of PF have been identified and tested as potential therapeutic targets [7]. Caveolin-1 (Cav-1) is an important functional protein of the caveolae that is highly expressed in the lungs and is required for maintaining the homeostatic functions of the pulmonary system [13]. In PF, reduced Cav-1 expression and function is associated with enhanced fibroblast proliferation, collagen

deposition, and inflammation [14, 15]. In the silicosis model mice, reduced levels of Cav-1 resulted in excessive accumulation of silica, which triggered excessive oxidative stress and lung fibrosis [16]. The role of Cav-1 in the anti-fibrotic effects of MSCs has been reported. Yao et al., demonstrated that MSCs from the human placenta (hPFMSCs) suppressed liver fibrosis in mice by upregulating Cav-1, which inhibited the TGF-β/Smad signaling pathway that was required for activation of the fibrotic genes [17]. Therefore, Cav-1 is a promising target for the suppression of PF by the MSCs including ADMSCs. In this study, we investigated the beneficial effects of ADMSCs in suppressing inflammation and fibrosis in the bleomycin-induced PF model rats and the underlying mechanisms by focusing on Cav-1-mediated pathways.

Methods

Isolation of the rat ADMSCs

Adult male SD rats (weighing 200 g –300 g) were purchased from the Labs & Centers of Sichuan West China School of Medicine, housed in the animal facility at constant room temperature (22-25^{o}C) and provided with food and water available *ad libitum*. All the animal experiments were performed in accordance with the guidelines proposed in the Guide for the Care and Use of Laboratory Animals (1985), NIH, Bethesda, USA, and were approved by the Ethics committee of the Guangzhou RuiGe Biotech Company (Guangzhou, China). To prepare the ADMSCs, the rats were anesthetized with isoflurane. Then, the adipose tissues surrounding the epididymis were carefully dissected, cut into 1–2 mm^3 size pieces, and digested with collagenase for 60 min at 37°C. Subsequently, the tissue clumps were dissociated by trituration with a 25-ml pipette for 2–3 min and filtered with a 70 μm nylon net. The cells were centrifuged at 157× g for 10 min and cultured in DMEM medium (SH30023.01B, HyClone, Carlsbad, USA) at 37°C in an atmosphere consisting of 5% CO_2 and 95% air for 24 h. The suspended cells were discarded and the adherent cells were used for further analysis and subsequent assays.

Characterization of the rat ADMSCs

The differentiation potential of the adherent cells was analyzed by Alizarin Red S (for osteogenic differentiation) and Oil Red O (for adipogenic differentiation) staining methods according to previously published protocols [18]. Briefly, for Alizarin Red S staining, the isolated adherent cells were washed twice with PBS and fixed in 3.7% paraformaldehyde at room temperature for 10 min. Then, the cells were incubated with 1% Alizarin Red (pH 4.2) for 10 min. Finally, the cells were washed twice with ddH_2O, dried, and photographed under a Leica INM200 UV microscope. The Oil Red O staining was performed by seeding the adherent cells in the adipogenic medium at a

density of 5×10^3 cells per well in a 12-well plate. Then, the cells were rinsed in PBS, fixed in 10% formalin, and incubated with 2% (wt/vol) Oil Red O reagent for 5 minutes at room temperature. The stained cells were examined under a light microscope and photographed. FACS analysis was performed to determine the stem cell characteristics of the potential ADMSCs by analyzing the expression of specific surface antigens such as CD29, CD34, CD44, CD45, and CD90 using a FACS flow cytometer (Accuri C6, BD, USA). The analysis was performed 30 minutes before transplantation.

Generation of bleomycin induced PF model rats and the ADMSC group rats

Eighteen rats were randomly distributed among the following three groups (n=6 per group): Control group, rats were injected intratracheally with 0.2 ml normal saline; PF group, rats were injected intratracheally with 5 mg/kg bleomycin sulfate (dissolved in 0.2 ml normal saline) (Merck, Darmstadt, Germany); ADMSC group, rats were generated by injecting a group of PF model mice with 0.5 ml ADMSCs (2.0×10^6) at 0, 12, and 24 hours after PF induction. The rats were sacrificed on day 21 after PF model establishment using 200 mg/kg of pentobarbital sodium. We harvested the lung tissues and extracted the bronchoalveolar lavage fluid (BALF) samples from all the rats for further analyses.

Collection of BALF

BALF was collected by flushing the left lungs of the sacrificed rats thrice with 2 ml PBS. The fluid was centrifuged at 1500 *g* for 10 min at 4ºC. The supernatant was collected as BALF and the BAL cell counts were estimated using a standard hemocytometer and expressed as eosinophils per 500 cells.

Hematoxylin-Eosin staining

The histology of right lungs was analyzed by staining with hematoxylin and eosin (H&E). Briefly, 3 μm thick formalin-fixed paraffin-embedded lung tissue sections were prepared and stained with H&E. The images were captured using an Olympus BX53 microscope (Olympus Lifesciences, Tokyo, Japan) at 400× magnification. The severity of the lung fibrosis was assessed according to the Ashcroft scale [19] with the following scoring criteria: 0 = normal lung; 1 = minimal fibrous thickening of the alveolar or bronchiolar walls, but no fibrotic masses present; 2 = moderate thickening of the walls without obvious damage to the lung architecture, but no fibrotic masses present; 3 = increased fibrosis with definite damage to the lung structure and the formation of fibrous bands or small fibrous masses; 4 = severe distortion of the structure and large fibrous areas (a honeycomb lung was placed

in this category); 5 = total fibrous obliteration of the lung tissue in the field; 6 = large contiguous fibrotic masses; 7 = alveoli nearly obliterated with fibrous masses; 8 = microscopic field with complete obliteration with fibrotic masses.

Enzyme-linked immune sorbent assay (ELISA) detection of cytokines, TGF-β1 and collagens

IL-6, IL-1β, and TGF-β1 levels in the supernatants of the lung tissues and the BALF samples were estimated using the corresponding ELISA kits (Nanjing Jiancheng Bioengineering Institute, China) according to the manufacturer's instructions. The supernatants of the lung tissues were prepared by grinding 1 g of fresh lung tissue under ice-cold conditions followed by centrifugation at 3,000 x g at 4˚C for 10 min. The levels of IL-6, IL-1β, and TGF-β1 in the supernatants were estimated using the ELISA kits.

Collagen I levels were analyzed in the lung tissue extract using the ELISA Kit (StressXpress from Assay Designs/Stressgen Bioreagents) according to the manufacturer's instructions.

Estimation of hydroxyproline in the lung tissues

Hydroxyproline levels in the lung tissues were estimated as previously reported. Briefly, the lung tissues were ground into fine powder, homogenized in RIPA buffer, and lyophilized for at least 24 h. Then, NaOH was added until the pH of the samples was 7.0. Then, the buffered samples were incubated for 20 min with 0.05M Chloramine T reagent. The reaction was terminated by incubating the samples with 70% perchloric acid for 20 min in a 55–65°C water bath. Then, Ehrlich's reagent was added to the samples. Hydroxyproline concentration in the samples was determined and expressed as μg of hydroxyproline per mg of protein

Western blotting assay

The whole cell proteins were extracted using the Total Protein Extraction Kit (Wanleibio, China) according to the manufacturer's instructions and quantified. Equal amounts of proteins were separated on an SDS-PAGE and transferred onto the PVDF membrane. Then, the membrane was blocked with 5% skimmed milk followed by incubation with primary and secondary antibodies. The protein blots were developed using Beyo ECL Plus reagent (Beyotime, China) with the Gel Imaging System. The relative expression levels of the proteins were calculated using GAPDH was used as internal reference protein. The primary antibody against NF-κB subunit p65 was purchased from Boster (BA0610. China). The primary antibodies against phosphorylated IκBα (p-IκBα; Cat. No. bs-5515R) and IκBα (Cat. No. bs-1287R) were purchased from Beijing Biosynthesis Biotechnology Co., Ltd.

(Beijing, China). The primary antibodies against Cav-1 (Cat. No. ab32577), GAPDH (Cat. No. ab8245), and Histone H3 (Cat. No. ab1791) were purchased from Abcam (China).

Electrophoretic mobility shift assay (EMSA)

EMSA was used to analyze the nuclear translocation of NF-κB p65. The nuclear proteins were extracted using the nuclear protein extraction kit. The super-shift EMSA assay was performed to determine the levels of DNA-bound p65 using the Electrophoretic mobility shift assay kit according to the manufacturer's instructions. The EMSA reaction mixture was subjected to electrophoresis at 180 V for 80 min and then developed with streptavidin-HRP (1:750) for 20 min at room temperature. The EMSA results were analyzed using the Gel-Pro-Analyzer (Media Cybernetics, USA).

Statistical analysis

Statistical analysis was performed using the GraphPad Prism version 6.0 software (GraphPad Software, Inc., San Diego, CA). The data are represented as mean ± standard deviation (SD). The statistical differences between the groups were analyzed using the One-way analysis of variance and post-hoc multiple comparisons using the Tukey's method. $P< 0.05$ (two tailed) was considered statistically significant.

Results

Isolation and characterization of the rat ADMSCs

The ADMSCs isolated from the rat adipose tissues showed positive Oil Red O staining, thereby demonstrating adipogenic differentiation potential (Figure 1A). They also showed positive Alizarin Red staining, thereby demonstrating osteogenic differentiation potential (Figure 1B). The stem cell feature of these cells was analyzed by flow cytometry. The third passage ADMSCs showed positive expression of cell surface markers, namely, CD29, CD44, and CD90, and absence of CD34 and CD45 expression on the cell surface ($CD29^+$ $CD44^+$ $CD90^+$ $CD34^-$ $CD45^-$) (Figure 1C). This demonstrated successful generation of the rat ADMSCs in our study.

ADMSCs attenuated bleomycin-induced injury and collagen accumulation in the lungs of the PF model rats

H&E staining results demonstrated significant higher lung permeability and excessive inflammatory cell infiltration in the lung tissues from the PF group compared to those from the control group, but these effects were

abrogated in the ADMSC group (Figure 2A). The Ashcroft score was significantly higher for the PF group compared to the ADMSC and the control groups. The BALF samples of the PF group rats showed significantly higher number of eosinophils compared to the control group rats ($P < 0.05$) (Figure 2B). Furthermore, the number of eosinophils were significantly reduced in the BALF samples of the ADMSC group compared to the BALF samples of the PF group ($P < 0.05$) (Figure 2B). ELISA assay results showed that bleomycin treatment significantly increased collagen I deposition in the lung tissues of the PF group compared to those from the control group, but collagen I deposition was suppressed by the ADMSCs ($P < 0.05$) (Figure 2C). We analyzed the levels of hydroxyproline to further confirm the excessive accumulation of collagen in the lung tissues of the PF group and the suppressive effects of ADMSCs. The hydroxyproline levels were significantly elevated in the lung tissues of the PF group rats but suppressed by the ADMSCs ($P < 0.05$) (Figure 2D).

ADMSCs attenuated the levels of pro-inflammatory cytokines in the bleomycin-induced PF model rats

Lung inflammation is the characteristic feature of PF progression. The levels of pro-inflammatory cytokines, namely, IL-6, IL-1β, and TGF-β1 were significantly higher in the lung tissues and BALF of the PF group rats compared to the control group rats ($P < 0.05$) (Figure 3). However, the ADMSC group rats showed significantly lower levels of IL-6, IL-1β, and TGF-β1 in the lung tissues and BALF compared to those of the PF group rats (Figure 3). This demonstrated that ADMSCs suppressed inflammation in the lung tissues of PF-induced rats. This also demonstrated the anti-fibrotic effects of the ADMSCs.

ADMSCs increased the levels of Cav-1 and inhibited the NF-κB signaling pathway in the PF model rats

We then analyzed the mechanisms underlying the anti-fibrotic effects of ADMSCs. As shown in Figure 4, the lung tissues of the PF group rats showed significantly lower levels of Cav-1 and IκBα and significantly higher levels of p-IκBα and nuclear p65 compared to the control group. This indicated activation of the pro-inflammatory NF-κB signaling pathway in the lungs of the PF group rats. However, the lung tissues of the ADMSC group rats showed higher levels of Cav-1 and IκBα and significantly lower levels of p-IκBα and nuclear p65 compared to the lung tissues of the PF group rats (Figure 4). EMSA results also confirmed that ADMSCs suppressed the translocation of NF-κB p65 subunit to the nucleus and its binding to the genomic DNA in the lung tissues of the bleomycin-induced PF model rats (Figure 5). These data further confirmed that the ADMSCs suppressed inflammation and fibrosis in the lungs of the PF model rats via the Cav-1/NF-kB axis.

Discussion

MSCs are generally isolated from the bone marrow, umbilical cord, blood, placenta, and adipose tissues of adult individuals [20-22]. They are characterized by multi-lineage differentiation capacity and show anti-apoptotic and anti-inflammatory properties [23-25]. In the clinic, MSCs from multiple sources have shown promising effects in the treatment of inflammatory and autoimmune diseases such as acute myocardial infarction and COPD. For instance, Xia et al. show that MSCs overexpressing farnesoid X receptor exert protective effects against acute ischemic myocardial injuries by binding endogenous bile acids [26]. Regarding pulmonary disorders, Abbaszadeh et al. summary the potential therapeutic effects and associated mechanisms of MSCs on COPDs [27]. Therefore, several studies are underway to evaluate the efficacy of MSCs in treating various human diseases. In the current study, we tested the efficacy of ADMSCs in suppressing the progression of PF in the rat model and analyzed the underlying mechanisms. Our data showed that ADMSCs isolated from the epididymis tissues of adult rats significantly attenuated tissue destruction, collagen deposition, and inflammatory response in the lungs of bleomycin-induced PF rats by the increasing the expression of Cav-1 and suppressing the NF-κB signaling pathway.

The therapeutic effects of ADMSCs on PF have been reported previously. Radwan et al showed that ADMSCs protected against amiodarone-induced lung injury in rats by inhibiting the proliferation of fibroblasts and the production of pro-fibrotic factors [28]. Furthermore, Shao et al demonstrated that ADMSCs repaired radiation-induced pulmonary fibrosis via a DKK-1-mediated Wnt/β-catenin pathway [29]. Our results also showed that ADMSCs reduced the infiltration of the neutrophils and the area of lung tissue injury by suppressing the production of collagen I and hydroxyproline and the levels of pro-inflammatory cytokines such as IL-6, IL-1β, and TGF-β1. Therefore, our data demonstrated the anti-fibrotic and anti-inflammatory effects of the ADMSCs in effectively suppressing bleomycin-induced PF in the rat model. We speculate that the anti-fibrotic effect of the ADMSCs may be related to their ability to suppress inflammation, which plays a key role in PF progression [30].

We also investigated the role of the Cav-1/NF-κB pathway in the anti-PF effects of the ADMSCs. Although previous studies have investigated the anti-PF functions of the ADMSCs, the underlying mechanisms have not been reported. Western blotting analysis demonstrated that the bleomycin treatment suppressed Cav-1 levels and enhanced activation of the NF-κB signaling pathway in the lung tissues of the PF group rats. However, these effects were abrogated by the ADSMCs. As reported previously, Cav-1 is a key regulator of lung fibrosis and inflammatory response. Cav-1 inhibited the infiltration of inflammatory cells and the secretion of cytokines in lungs of lipopolysaccharide (LPS)-stimulated mice [31, 32]. The anti-PF effects of Cav-1 are exerted via multiple

pathways. For example, the up-regulation of Cav-1 attenuates rat pulmonary arterial hypertension by inhibiting the TGF-β1/Smad signaling pathway [33]. Liu et al. showed that up-regulation of Cav-1 expression by dexmedetomidine attenuated LPS-induced lung injury by suppressing the pro-inflammatory TLR4/NF-κB signaling pathway [32]. Moreover, Cav-1 inhibited silica-induced infiltration of the immune cells and secretion of inflammatory factors by downregulating the NF-κB signaling pathway [16]. The interaction between Cav-1 and the pro-inflammatory NF-κB pathway has been well-characterized. Ohnuma et al reported that the CD26/Cav-1 interaction on the TT-loaded monocytes resulted in the phosphorylation of Cav-1 and subsequent activation of NF-κB [34]. Xu et al reported that dexmedetomidine alleviated pulmonary inflammation after intestinal ischemia-reperfusion injury by promoting Cav-1 expression and subsequent inhibition of p38 and NF-kB signaling [32]. Li et al reported that Wilms' tumor 1-associating protein (WTAP) facilitated the progression of endometrial cancer through the Cav-1/NF-κB signaling axis [35, 36]. The selective inhibition of NF-κB pathway has been reported to attenuate lung injuries by multiple previous studies [37-39]. Our results also demonstrate that the anti-PF effects of the ADMSCs involves the up-regulation of Cav-1 and inhibition of NF-κB, thereby attenuating the inflammatory response related to bleomycin-induced PF. Except for modulating the activity of NF-κB signaling axis, other downstream effectors of Cav-1, such as Pink-1/Parkin pathway [40], are also involved in the fibrosis of other organs [41, 42]. Thus, further exploration is also needed in the future to provide more detail explanation on the role of Cav-1 in the anti-PF function of ADMSCs.

In conclusion, this study demonstrated that the ADMSCs suppressed lung inflammation and fibrosis in the bleomycin-induced PF model rats via the Cav-1/NF-κB pathway. Further pre-clinical and clinical studies are necessary to confirm our findings regarding the beneficial effects of the ADMSCs in the treatment of human lung disorders including PF.

Declarations

Funding

Not applicable

Competing interests

The authors disclose no conflict of interest

Author Contributions

All authors contributed to the study conception and design. Material preparation, data collection and analysis were performed by Zhe Chen, Bingqing Ruan, and Guangyan Long. The first draft of the manuscript was written by Zhe Chen and Weil Lin. All authors commented on previous versions of the manuscript. All authors read and approved the final manuscript.

Ethics approval

All the animal experiments were performed in accordance with international guidelines for care and use of laboratory animals and approved by the ethic committee of Sichuan West China School of Medicine.

Consent to participate

Not applicable

Consent to publish

Not applicable

Acknowledgements

Not applicable

References

1. Ware LB, Matthay MA. The acute respiratory distress syndrome. N Engl J Med. 2000;342(18):1334-49. doi:10.1056/nejm200005043421806.

2. Perez A, Rogers RM, Dauber JH. The prognosis of idiopathic pulmonary fibrosis. Am J Respir Cell Mol Biol. 2003;29(3 Suppl):S19-26.

3. Chlumský J, Stehlík L, Šterclová M, Smetanová J, Zindr O. Exercise Tolerance in Patients With Idiopathic Pulmonary Fibrosis, Effect of Supplemental Oxy-Gen. Physiol Res. 2022;71(2):317-21. doi:10.33549/physiolres.934764.

4. American Thoracic Society. Idiopathic pulmonary fibrosis: diagnosis and treatment. International consensus statement. American Thoracic Society (ATS), and the European Respiratory Society (ERS). Am J Respir Crit Care Med. 2000;161(2 Pt 1):646-64. doi:10.1164/ajrccm.161.2.ats3-00.

5. Raghu G. Idiopathic pulmonary fibrosis: treatment options in pursuit of evidence-based approaches. Eur Respir J. 2006;28(3):463-5. doi:10.1183/09031936.06.00086606.

6. Sime PJ, Xing Z, Graham FL, Csaky KG, Gauldie J. Adenovector-mediated gene transfer of active transforming growth factor-beta1 induces prolonged severe fibrosis in rat lung. J Clin Invest. 1997;100(4):768-76. doi:10.1172/jci119590.

7. Scotton CJ, Chambers RC. Molecular targets in pulmonary fibrosis: the myofibroblast in focus. Chest. 2007;132(4):1311-21. doi:10.1378/chest.06-2568.

8. Sueblinvong V, Weiss DJ. Stem cells and cell therapy approaches in lung biology and diseases. Transl Res. 2010;156(3):188-205. doi:10.1016/j.trsl.2010.06.007.

9. Ortiz LA, Gambelli F, McBride C, Gaupp D, Baddoo M, Kaminski N et al. Mesenchymal stem cell engraftment in lung is enhanced in response to bleomycin exposure and ameliorates its fibrotic effects. Proc Natl Acad Sci U S A. 2003;100(14):8407-11. doi:10.1073/pnas.1432929100.

10. Periera-Simon S, Xia X, Catanuto P, Coronado R, Kurtzberg J, Bellio M et al. Anti-fibrotic effects of different sources of MSC in bleomycin-induced lung fibrosis in C57BL6 male mice. Respirology. 2021;26(2):161-70. doi:10.1111/resp.13928.

11. Leu S, Lin YC, Yuen CM, Yen CH, Kao YH, Sun CK et al. Adipose-derived mesenchymal stem cells markedly attenuate brain infarct size and improve neurological function in rats. J Transl Med. 2010;8:63. doi:10.1186/1479-5876-8-63.

12. Banas A, Teratani T, Yamamoto Y, Tokuhara M, Takeshita F, Osaki M et al. IFATS collection: in vivo

therapeutic potential of human adipose tissue mesenchymal stem cells after transplantation into mice with liver injury. Stem Cells. 2008;26(10):2705-12. doi:10.1634/stemcells.2008-0034.

13. Sanon VP, Sawaki D, Mjaatvedt CH, Jourdan-Le Saux C. Myocardial tissue caveolae. Compr Physiol. 2015;5(2):871-86. doi:10.1002/cphy.c140050.

14. Gvaramia D, Blaauboer ME, Hanemaaijer R, Everts V. Role of caveolin-1 in fibrotic diseases. Matrix Biol. 2013;32(6):307-15. doi:10.1016/j.matbio.2013.03.005.

15. Kulshrestha R, Singh H, Pandey A, Mehta A, Bhardwaj S, Jaggi AS. Caveolin-1 as a critical component in the pathogenesis of lung fibrosis of different etiology: Evidences and mechanisms. Exp Mol Pathol. 2019;111:104315. doi:10.1016/j.yexmp.2019.104315.

16. He R, Yuan X, Lv X, Liu Q, Tao L, Meng J. Caveolin-1 negatively regulates inflammation and fibrosis in silicosis. J Cell Mol Med. 2021. doi:10.1111/jcmm.17045.

17. Yao Y, Xia Z, Cheng F, Jang Q, He J, Pan C et al. Human placental mesenchymal stem cells ameliorate liver fibrosis in mice by upregulation of Caveolin1 in hepatic stellate cells. Stem Cell Res Ther. 2021;12(1):294. doi:10.1186/s13287-021-02358-x.

18. Li F, Niyibizi C. Cells derived from murine induced pluripotent stem cells (iPSC) by treatment with members of TGF-beta family give rise to osteoblasts differentiation and form bone in vivo. BMC Cell Biol. 2012;13:35. doi:10.1186/1471-2121-13-35.

19. Ashcroft T, Simpson JM, Timbrell V. Simple method of estimating severity of pulmonary fibrosis on a numerical scale. J Clin Pathol. 1988;41(4):467-70. doi:10.1136/jcp.41.4.467.

20. Roshandel E, Mehravar M, Dehghani Ghorbi M, Tabarraee M, Salimi M, Hajifathali A. Potential and challenges of placenta-derived decidua stromal cell therapy in inflammation-associated disorders. Hum Immunol. 2022;83(7):580-8. doi:10.1016/j.humimm.2022.04.011.

21. Itro A, Trotta MC, Miranda R, Paoletta M, De Cicco A, Lepre CC et al. Why Use Adipose-Derived Mesenchymal Stem Cells in Tendinopathic Patients: A Systematic Review. Pharmaceutics. 2022;14(6). doi:10.3390/pharmaceutics14061151.

22. Ding N, Li E, Ouyang X, Guo J, Wei B. The Therapeutic Potential of Bone Marrow Mesenchymal Stem Cells for Articular Cartilage Regeneration in Osteoarthritis. Curr Stem Cell Res Ther. 2021;16(7):840-7. doi:10.2174/1574888x16666210127130044.

23. Gu C, Zhang H, Zhao S, He D, Gao Y. Mesenchymal Stem Cell Exosomal miR-146a Mediates the Regulation of the TLR4/MyD88/NF-κB Signaling Pathway in Inflammation due to Diabetic Retinopathy. Comput Math

Methods Med. 2022;2022:3864863. doi:10.1155/2022/3864863.

24. Basir HRG, Karbasi A, Ravan AP, Abbasalipourkabir R, Bahmani M. Is human umbilical cord mesenchymal stem cell-derived conditioned medium effective against oxidative and inflammatory status in CCl(4)- induced acute liver injury? Life Sci. 2022:120730. doi:10.1016/j.lfs.2022.120730.

25. Liu H, Shi M, Li X, Lu W, Zhang M, Zhang T et al. Adipose Mesenchymal Stromal Cell-Derived Exosomes Prevent Testicular Torsion Injury via Activating PI3K/AKT and MAPK/ERK1/2 Pathways. Oxid Med Cell Longev. 2022;2022:8065771. doi:10.1155/2022/8065771.

26. Xia Y, Xu X, Guo Y, Lin C, Xu X, Zhang F et al. Mesenchymal Stromal Cells Overexpressing Farnesoid X Receptor Exert Cardioprotective Effects Against Acute Ischemic Heart Injury by Binding Endogenous Bile Acids. Adv Sci (Weinh). 2022:e2200431. doi:10.1002/advs.202200431.

27. Abbaszadeh H, Ghorbani F, Abbaspour-Aghdam S, Kamrani A, Valizadeh H, Nadiri M et al. Chronic obstructive pulmonary disease and asthma: mesenchymal stem cells and their extracellular vesicles as potential therapeutic tools. Stem Cell Res Ther. 2022;13(1):262. doi:10.1186/s13287-022-02938-5.

28. Radwan SM, Ghoneim D, Salem M, Saeed M, Saleh Y, Elhamy M et al. Adipose Tissue-Derived Mesenchymal Stem Cells Protect Against Amiodarone-Induced Lung Injury in Rats. Appl Biochem Biotechnol. 2020;191(3):1027-41. doi:10.1007/s12010-020-03227-8.

29. Shao L, Zhang Y, Shi W, Ma L, Xu T, Chang P et al. Mesenchymal stromal cells can repair radiation-induced pulmonary fibrosis via a DKK-1-mediated Wnt/β-catenin pathway. Cell Tissue Res. 2021;384(1):87-97. doi:10.1007/s00441-020-03325-3.

30. Nie YJ, Wu SH, Xuan YH, Yan G. Role of IL-17 family cytokines in the progression of IPF from inflammation to fibrosis. Mil Med Res. 2022;9(1):21. doi:10.1186/s40779-022-00382-3.

31. Cai L, Yi F, Dai Z, Huang X, Zhao YD, Mirza MK et al. Loss of caveolin-1 and adiponectin induces severe inflammatory lung injury following LPS challenge through excessive oxidative/nitrative stress. Am J Physiol Lung Cell Mol Physiol. 2014;306(6):L566-73. doi:10.1152/ajplung.00182.2013.

32. Liu J, Huang X, Hu S, He H, Meng Z. Dexmedetomidine attenuates lipopolysaccharide induced acute lung injury in rats by inhibition of caveolin-1 downstream signaling. Biomed Pharmacother. 2019;118:109314. doi:10.1016/j.biopha.2019.109314.

33. Gao W, Shao R, Zhang X, Liu D, Liu Y, Fa X. Up-regulation of caveolin-1 by DJ-1 attenuates rat pulmonary arterial hypertension by inhibiting TGFβ/Smad signaling pathway. Exp Cell Res. 2017;361(1):192-8. doi:10.1016/j.yexcr.2017.10.019.

34. Ohnuma K, Inoue H, Uchiyama M, Yamochi T, Hosono O, Dang NH et al. T-cell activation via CD26 and caveolin-1 in rheumatoid synovium. Mod Rheumatol. 2006;16(1):3-13. doi:10.1007/s10165-005-0452-4.

35. Xu L, Li T, Chen Q, Liu Z, Chen Y, Hu K et al. The α2AR/Caveolin-1/p38MAPK/NF-κB axis explains dexmedetomidine protection against lung injury following intestinal ischaemia-reperfusion. J Cell Mol Med. 2021;25(13):6361-72. doi:10.1111/jcmm.16614.

36. Li Q, Wang C, Dong W, Su Y, Ma Z. WTAP facilitates progression of endometrial cancer via CAV-1/NF-κB axis. Cell Biol Int. 2021;45(6):1269-77. doi:10.1002/cbin.11570.

37. Kopincova J, Mikolka P, Kolomaznik M, Kosutova P, Calkovska A, Mokra D. Selective inhibition of NF-kappaB and surfactant therapy in experimental meconium-induced lung injury. Physiol Res. 2017;66(Suppl 2):S227-s36. doi:10.33549/physiolres.933678.

38. Liu L, Chen X, Jiang Y, Yuan Y, Yang L, Hu Q et al. Brevilin A Ameliorates Acute Lung Injury and Inflammation Through Inhibition of NF-κB Signaling via Targeting IKKα/β. Front Pharmacol. 2022;13:911157. doi:10.3389/fphar.2022.911157.

39. Guo H, Song Y, Li F, Fan Y, Li Y, Zhang C et al. ACT001 suppressing M1 polarization against inflammation via NF-κB and STAT1 signaling pathways alleviates acute lung injury in mice. Int Immunopharmacol. 2022;110:108944. doi:10.1016/j.intimp.2022.108944.

40. Jiang W, Wang J, Xue W, Xin J, Shi C, Wen J et al. Caveolin-1 attenuates acetaminophen aggravated lipid accumulation in alcoholic fatty liver by activating mitophagy via the Pink-1/Parkin pathway. Eur J Pharmacol. 2021;908:174324. doi:10.1016/j.ejphar.2021.174324.

41. Dou SD, Zhang JN, Xie XL, Liu T, Hu JL, Jiang XY et al. MitoQ inhibits hepatic stellate cell activation and liver fibrosis by enhancing PINK1/parkin-mediated mitophagy. Open Med (Wars). 2021;16(1):1718-27. doi:10.1515/med-2021-0394.

42. Ma N, Wei Z, Hu J, Gu W, Ci X. Farrerol Ameliorated Cisplatin-Induced Chronic Kidney Disease Through Mitophagy Induction via Nrf2/PINK1 Pathway. Front Pharmacol. 2021;12:768700. doi:10.3389/fphar.2021.768700.

Figure Legends

Figure 1. Characterization of the rat ADMSCs. (A) Oil red O assay results show the adipogenic differentiation potential of the rat ADMSCs. (**B**) Alizarin red assay results show the osteogenic differentiation of the rat ADMSCs. (**C)** FACS analysis results show the cell surface expression levels of CD34, CD45, CD29, CD44, and CD90 in the rat ADMSCs.

Figure 2 Effects of ADMSCs on the lung structure, inflammation, and fibrosis in the bleomycin-induced PF model rats. (**A)** H&E staining results demonstrate the histology of the lung tissues in the control, PF, and ADMSC group rats. **(B)** The number of eosinophils in the BALF of the control, PF, and ADMSC group rats. **(C)** ELISA results demonstrate the levels of collagen I in the lung tissues of the control, PF, and ADMSC group rats. (**D)** The hydroxyproline (Hyp) levels in the lung tissues of the control, PF, and ADMSC group rats. * denotes $P < 0.05$ compared with the control group; $^{\#}$ denotes $P < 0.05$ compared with the PF group.

Figure 3. Effects of ADMSCs on the production of pro-inflammatory cytokines in the lung tissues and the BALF of the bleomycin-induced PF model rats. (A-C) ELISA results demonstrate the levels of **(A)** IL-6, (**B)** IL-1β and (**C)** TGF-β1 in the lung tissues of the control, PF, and ADMSC group rats. **(D-F)** ELISA results show the levels of (D) IL-6, (**E)** IL-1β, and (**F)** TGF-β1 in the BALF of the control, PF, and the ADMSC group rats. * denotes $P < 0.05$ compared with the control group; $^{\#}$ denotes $P < 0.05$ compared with the PF group.

Figure 4. Effects of ADMSCs on the expression levels of Cav-1 and activity of the NF-κB signaling pathway in the lung tissues of the bleomycin-induced PF model rats. Representative images of the western blots and the corresponding statistical analyses show the levels of Cav-1, IκBα, p-IκBα, and nuclear p65 in the lung tissues of the control, PF, and ADMSC group rats. * denotes $P < 0.05$ compared with the control group; $^{\#}$ denotes $P < 0.05$ compared with the PF group.

Figure 5. Effects of ADMSCs on the nuclear translocation of p65 in lung tissues of the bleomycin-induced PF model rats. Representative western blots and the corresponding statistical analyses show the nuclear translocation status of p65 protein in the lung tissues of the control, PF, and ADMSC group rats. * denotes $P < 0.05$ compared with the control group; $^{\#}$ denotes $P < 0.05$ compared with the PF group.

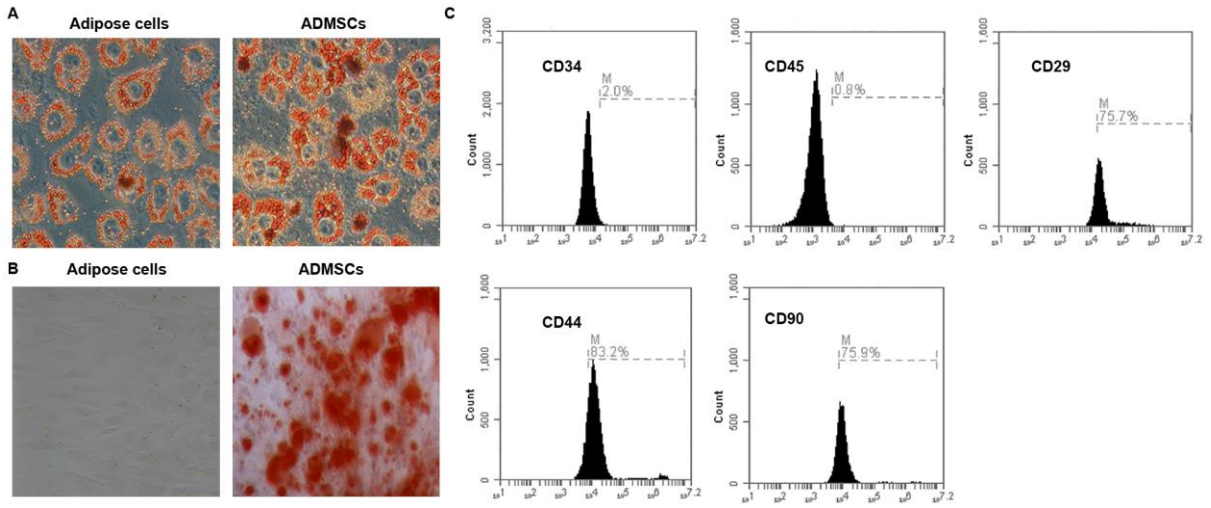
A
Adipose cells
ADMSCs
B
Adipose cells
ADMSCs
C
CD34
M
2.0%
CD45
M
0.8%
CD29
M
75.7%
CD44
M
83.2%
CD90
M
75.9%
Count

Fig. 1

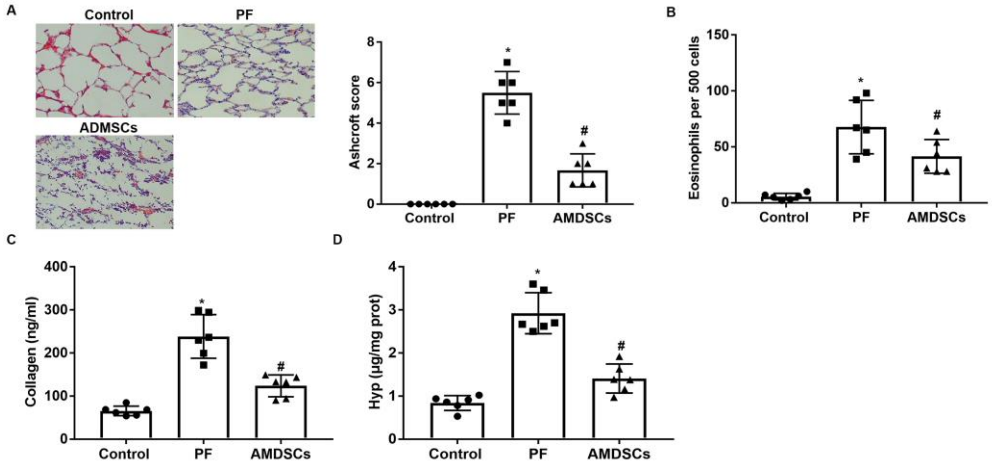
A
Control
PF
ADMSCs
Ashcroft score
B
Eosinophils per 500 cells
C
Collagen (ng/ml)
D
Hyp (μg/mg prot)
Control
PF
AMDSCs

Fig. 2

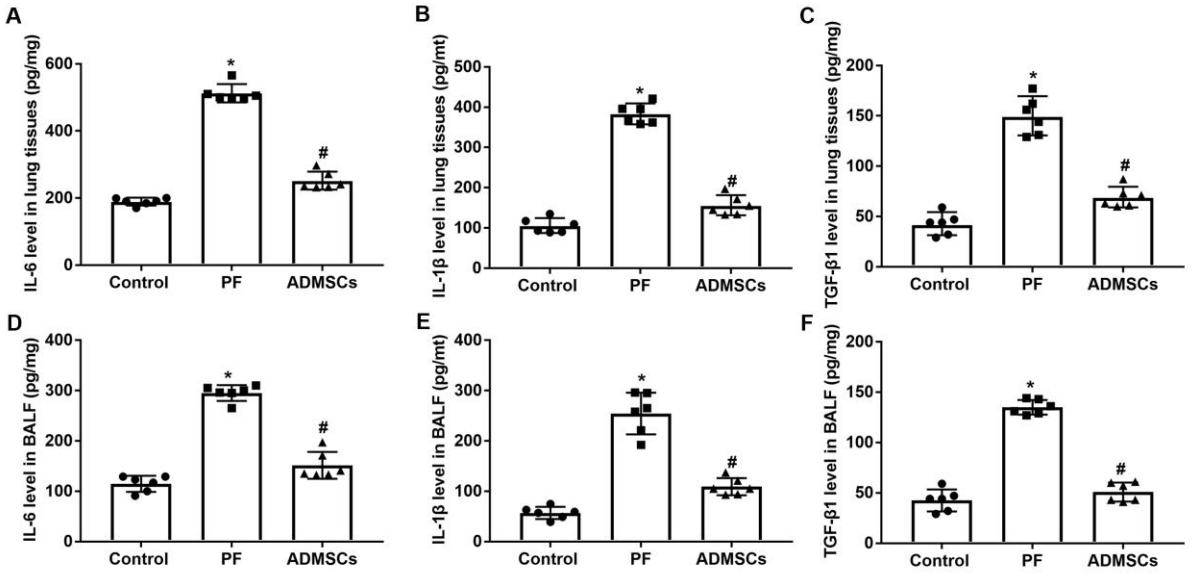

Fig. 3

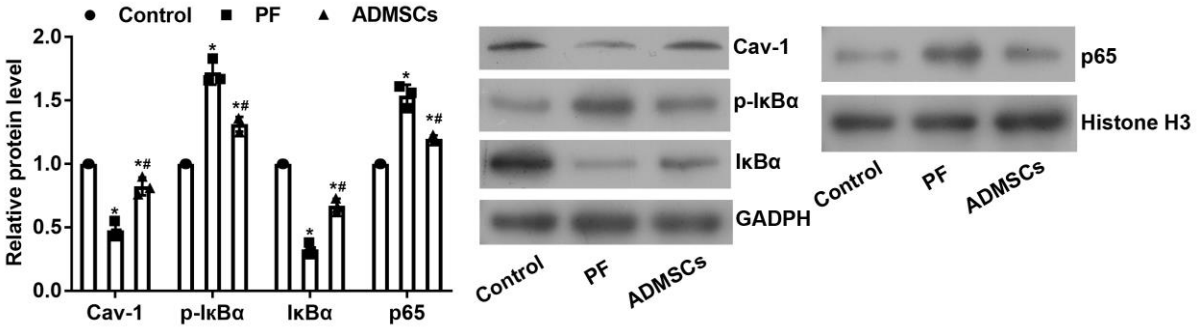

Fig. 4

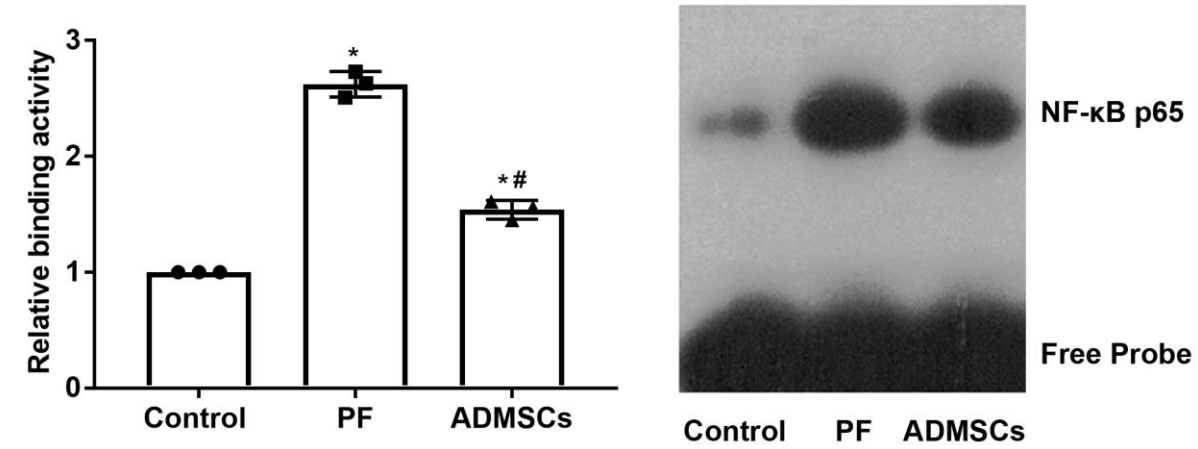

Fig. 5